8-2016

Tailoring Plate Thickness of a Helmholtz Resonator for Improved Sound Attenuation

Shahin Nudehi
Valparaiso University, shahin.sabokdasnudehi@valpo.edu

Scott Duncan
Valparaiso University, Scott.Duncan@valpo.edu

Recommended Citation
Kurdi, M., Nudehi, S., and Duncan, G.S. (2016). Tailoring plate thickness of a Helmholtz resonator for improved sound attenuation. Proceedings of the ASME 2016 International Design Engineering Technical Conferences & Computers and Information in Engineering Conference IDETC/CIE, North Carolina.

IDETC2016-59302 TAILORING PLATE THICKNESS OF A HELMHOLTZ RESONATOR FOR IMPROVED SOUND…

Conference Paper · August 2016

DOI: 10.1115/DETC2016-59302

4 authors, including:

Mohammad Kurdi
Ford Motor Company
32 PUBLICATIONS **231** CITATIONS

SEE PROFILE

Proceedings of the ASME 2016 International Design Engineering Technical Conferences & Computers and Information in Engineering Conference
IDETC/CIE 2016
August 21-24, 2016, North Carolina, USA

IDETC2016-59302

TAILORING PLATE THICKNESS OF A HELMHOLTZ RESONATOR FOR IMPROVED SOUND ATTENUATION

Dr. Mohammad Kurdi
Power Transmission Division
Lufkin Industries, LLC
Part of GE Oil and Gas
Wellsvile, NY 14895
Email: mohammad.kurdi@ge.com

Dr. Shahin Nudehi*
Mechanical Engineering Dept.
Valparaiso University
Valparaiso, Indiana, 46383
Email: shahin.nudehi@valpo.edu

Dr. Gregory Scott Duncan
Mechanical Engineering Dept.
Valparaiso University
Valparaiso, Indiana, 46383
Email: scott.duncan@valpo.edu

ABSTRACT

A Helmholtz resonator with flexible plate attenuates noise in exhaust ducts, and the transmission loss function quantifies the amount of filtered noise at a desired frequency. In this work the transmission loss is maximized (optimized) by allowing the resonator end plate thickness to vary for two cases: 1) a non-optimized baseline resonator, and 2) a resonator with a uniform flexible endplate that was previously optimized for transmission loss and resonator size. To accomplish this, receptance coupling techniques were used to couple a finite element model of a varying thickness resonator end plate to a mass-spring-damper model of the vibrating air mass in the resonator. Sequential quadratic programming was employed to complete a gradient based optimization search. By allowing the end plate thickness to vary, the transmission loss of the non-optimized baseline resonator was improved significantly, 28 percent. However, the transmission loss of the previously optimized resonator for transmission loss and resonator size showed minimal improvement.

1 Introduction

Due to their use in aerospace, automotive, and industrial applications for sound attenuation or the generation of sound vibration, there is a continued interest in acoustic devices. Therefore, a need exists for analysis and design tools that can be used in the development of new products or the improvement of existing products.

Investigators have previously applied analytical and optimization techniques to the development of acoustic devices. In an effort to develop flat loudspeakers, Doaré et al. [5] derived a dynamic model of a circular clamped plate in the presence of excitations from a voice coil and piezoelectric patches. An optimization study was carried out to design the geometry of the voice coil and patches to maximize the amplitude of the first mode while minimizing the amplitude at other modes. Duan et al. [6] considered improving the response of circular plates with free edges by altering their thickness. An analytical model was derived to model the stepped plate and a higher thickness at the boundary was found to produce a favorable symmetric mode similar to clamped plates.

Prior work also includes efforts to improve device response, which depends on the alignment of the actuation with the structure resonant frequencies. Peters et al. [13] utilized eigenmode sensitivities to identify preferable locations in the structure to improve system response. Additional work [12] includes the identification of temporary changes in the structure to minimize power consumption.

This work presents a continuation of the author's effort to improve the sound attenuation of passive Helmholtz resonators with a flexible circular plate. Previously, Nudehi, et. al. [11] created an analytical model of a passive Helmholtz resonator with a flexible uniform thickness circular end plate using receptance coupling techniques [2]. Kurdi, et. al. [8] used this analytical model

*Address all correspondence to this author.

in conjunction with a gradient based optimization search to optimize a baseline resonator with a flexible endplate to achieve a maximum transmission loss at a desired frequency while minimizing the resonator size.

In this paper, the authors expand upon their previous work to include in the optimization a flexible endplate that can vary in thickness throughout its area. Two questions are investigated: how much can a flexible endplate with optimized, varying endplate thickness 1) improve the transmission loss of the baseline resonator (with no other changes to geometry) and 2) improve the transmission loss of a resonator with a uniform thickness flexible endplate previously optimized for transmission loss and minimum resonator size.

To accomplish this a numerical model of the transmission loss function of the resonator is derived by coupling a finite element model (FEM) of the top circular endplate [1] with single-degree-of-freedom model of the acoustic field in the resonator chamber. Coupling is achieved through receptance coupling substructure analysis [2]. An analysis and design framework of the resonator is developed within the Finite Element Analysis Program (FEAP) environment [15]. Adjoint design sensitivities of the transmission loss are derived to expedite the gradient-based optimization search, which is carried out using sequential quadratic programming method utilizing NLPQLP library [14].

The paper is organized as follows. The optimization problem is formulated in Sections 2 and 3. The transmission loss and adjoint sensitivity of a Helmholtz resonator with a flexible plate are provided in Sections 4 and 5. The verification and optimization results for the model and sensitivity are provided in Section 6, and the conclusions are presented in Section 7.

2 Summary of Previous Work: Transmission Loss Optimization of a Helmholtz Resonator with a Uniform Thickness Flexible Plate

In our previous study, a design process was introduced to produce small volume Helmholtz resonators with flexible uniform thickness plates capable of achieving high transmission loss across a specified frequency range [8]. Figure 1 shows the geometry of the resonator with the flexible plate. For the design process, a multi-objective optimization procedure was applied in which the resonator's cavity volume and transmission loss were considered as the two competing objectives. The outcome of the optimization was the geometry of the resonator (neck diameter, neck length, cavity diameter, cavity height) and the thickness of the flexible plate, which was assumed to be uniform. In this paper, we refer to this optimization as the level-1 optimization, in which the optimal resonator's parameters and the thickness of flexible plate were determined to achieve high transmission loss across a specified frequency range.

The optimization produced a Pareto curve of potential resonator and plate designs, allowing the designer to select a design from

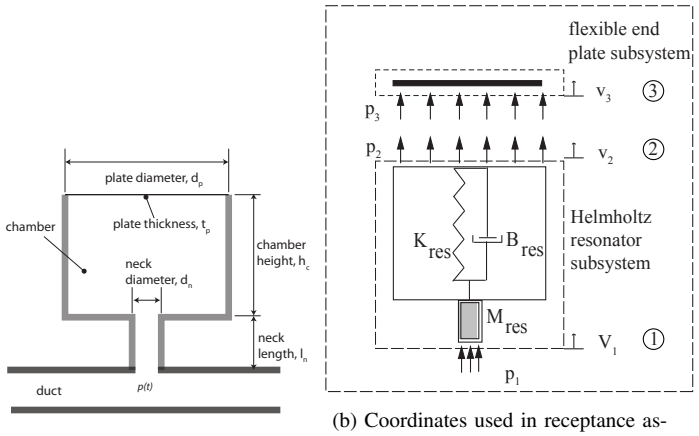

(a) Geometric properties

(b) Coordinates used in receptance assembly

FIGURE 1: Helmholtz resonator with a flexible plate

a variety of optimal designs that meets the designer's particular size and transmission loss specifications. One of the level-1 optimization results (Optimal Design-1) is shown in Table 1. Also, Table 1 shows the geometric properties of a baseline, non-optimized Helmholtz resonator design with a flexible end plate (studied in [11]). The baseline resonator has a transmission loss peak at a frequency of 30 Hz, the desired frequency chosen in the optimal design formulation. Also, in the level-1 optimization, the baseline geometry was used as the start of the search to find the optimal resonator geometry.

Quantity	d_p(mm)	t_p(mm)	d_n(mm)	l_n(mm)	h_c(mm)	ΔTL(dB)
Baseline	194.31	0.254	18.67	19.25	200.00	6.83
Optimal Design-1	203.20	0.2413	20.32	9.52	81.28	10.23

TABLE 1: Resonator geometric properties.

In Table 1, the flexible plate diameter is d_p, t_p is the flexible plate thickness, d_n is the resonator neck diameter, l_n is the resonator neck length, h_c is the resonator chamber height, and ΔTL is the weighted transmission loss. The geometrical variables are shown in Figure 1a.

3 Analytical Development: Transmission Loss Optimization of a Helmholtz Resonator with a Non-Uniform Thickness Flexible Plate

3.1 Optimization Objective and Constraint

The goal of the optimization search is to provide the highest transmission loss across the specified frequency range. To accomplish this we permit the flexible plate thickness to be non-

uniform, and the design variable vector in the optimization problem only includes the thickness of each material element in the finite element mesh of the plate. The transmission loss objective function is formulated in (8) and shown below:

$$\min_{b} \quad \Delta TL = -\frac{TL(\omega_{\text{desired}}-\delta)+\alpha TL(\omega_{\text{desired}})+TL(\omega_{\text{desired}}+\delta)}{2+\alpha} \tag{1}$$

where, $TL(\omega_{\text{desired}})$ is the transmission loss at selected frequency, ω_{desired} is the nominal selected frequency, δ is the selected frequency band around ω_{desired}, α is a weighting factor to favor ω_{desired}, and ΔTL is the weighted transmission loss. The objective function creates a desired frequency band in which the maximum transmission loss will occur and is weighted such that the maximum transmission loss is directed to the center of the band.

The objective function is constrained by the following:

$$g = \sum_{i=1}^{ndv} A^{(i)} t_p^{(i)} - \frac{\pi d_p^2}{4} t_p \leq 0.0, \tag{2}$$

where g is the constraint, $A^{(i)}$ is the area of the i^{th} element in the plate finite element mesh, design vector b includes the elements thickness ($t_p^{(i)}$), t_p and d_p are the plate thickness and diameter of the non-optimized resonator, respectively, and ndv is the number of elements used in the plate mesh. The constraint is applied such that the volume of the optimized, non-uniform plate is equal to or less than the volume of the non-optimized, uniform plate. The purpose of the constraint is to provide an optimized resonator with a weight equal to or less than the non-optimized resonator.

4 Analysis Model

The transmission loss of the resonator is defined as [4]:

$$TL = 20\log_{10}|\beta| \tag{3}$$

where

$$\beta = 1 + i\omega H(\omega)\frac{\rho a}{2A_{duct}} \tag{4}$$

and $H(\omega)$ is the frequency response of the resonator assembly, ω is the excitation frequency, ρ is the air density, a is the speed of sound and A_{duct} is the cross-sectional area of the duct where the resonator is installed. $H(\omega)$ is derived by coupling the frequency response function of the flexible end plate and the standard Helmholtz resonator using the receptance coupling method. The result of the coupling is summarized in (5)

$$H = h_{11}(\omega) - \frac{h_{12}(\omega)h_{21}(\omega)}{h_{22}(\omega)+h_{33}(\omega)} \tag{5}$$

In this equation, $h_{11}(\omega)$ is the direct receptance of the Helmholtz resonator subsystem at coordinate 1, $h_{22}(\omega)$ is the direct receptance of the Helmholtz resonator at coordinate 2, $h_{33}(\omega)$ is the direct receptance of the flexible end plate subsystem at coordinate 3, and $h_{21}(\omega) = h_{12}(\omega)$ is the cross receptance of the Helmholtz resonator subsystem at the coordinates 1 and 2. Figure 1b displays the coordinates in relation to the resonator and plate. Assuming a harmonic input pressure, the expressions for these receptances are:

$$h_{11}(\omega) = \frac{v_1}{p_1} = \frac{-1}{\omega^2 M_{\text{res}}} \tag{6a}$$

$$h_{22}(\omega) = \frac{v_2}{p_2} = \frac{\omega^2 M_{\text{res}} - i\omega B_{\text{res}} - K_{\text{res}}}{\omega^2(i\omega M_{\text{res}} B_{\text{res}} + M_{\text{res}} K_{\text{res}})} \tag{6b}$$

$$h_{33}(\omega) = \frac{v_3}{p_3} \tag{6c}$$

$$h_{12}(\omega) = \frac{v_1}{p_2} = \frac{-1}{\omega^2 M_{\text{res}}} \tag{6d}$$

In (6) p_j and v_j are the pressure and displaced volume at coordinate j, $i = \sqrt{-1}$, B_{res} is the equivalent viscous damping of the resonator [16], and M_{res} , K_{res}, are the equivalent resonator mass and stiffness, respectively, which are defined below:

$$M_{\text{res}} = \frac{m_{\text{neck}}}{A_{\text{neck}}^2} \tag{7a}$$

$$K_{\text{res}} = \frac{\rho a^2}{V}_{\text{chamber}} \tag{7b}$$

where m_{neck} is the mass of the fluid in the neck and A_{neck} is the cross-sectional area of the neck.

The receptance of (6c) is found by considering the finite element model of plate. Equations of motion of the plate are derived by considering the principle of virtual work [7].

$$[M]\,\ddot{q}(t) + (i\gamma + 1)\,[K]\,q(t) = f. \tag{8}$$

Here $\ddot{q}(t)$ is the global nodal deformation vector, $[M]$ is the global mass matrix, $[K]$ is the global stiffness matrix, f is the external

force vector, γ is structural damping factor. The damping contribution is derived by assuming the internal friction of the plate depends on the response amplitude only, is independent of excitation frequency and is proportional to the stiffness matrix [10]. Applying expansion theorem [10] one can transform (8) into modal coordinates by substituting the modal approximation:

$$q(t) = \sum_{r=1}^{n} \eta_r(t) u_r \tag{9}$$

to yield

$$\ddot{\eta}(t) + (i\gamma + 1)[\Lambda]\eta(t) = [U]^T f \tag{10}$$

In the above equations, u_r is the r^{th} mode shape of the plate with a modal deformation of $\eta_r(t)$, n is the number of modes in the eigensolution of the plate, η is modal deformation vector of size n, $[U]$ is the matrix of eigenvectors normalized to the mass matrix [3], and $[\Lambda]$ is the diagonal matrix of the plate natural frequencies (ω_r) which are the results of the below eigenvalue problem:

$$[K]u_r = \mu_r [M] u_r \tag{11}$$

where $\mu_r = \omega_r^2$.
Utilizing the mode shapes, the displaced plate volume in (6c) is computed by integrating (9) over the plate area

$$v_3(t) = \sum_{r=1}^{n} \eta_r(t) \int_A u_r \mathrm{d}A = \sum_{r=1}^{n} \eta_r(t) u_r^T A \tag{12}$$

where A is a column vector consisting of the plate mesh elements area.
The plate receptance is then found by transferring (10) into the frequency domain by substituting $\eta = \delta\eta \exp(i\omega t)$ and $f = \delta f \exp(i\omega t)$. This will result in:

$$\delta\eta_r = \frac{u_r^T \delta f}{(i\gamma+1)\omega_r^2 - \omega^2} \tag{13}$$

Substituting the expression for η_r in the frequency domain from (13) into (12), will yield the displaced volume of the resonator plate in the frequency domain as shown below:

$$\delta v_3 = \sum_{r=1}^{n} \frac{u_r^T A u_r^T \delta f}{(i\gamma+1)\omega_r^2 - \omega^2} \tag{14}$$

5 Adjoint Sensitivity

In the optimization, calculating the sensitivity using standard finite differences is computationally costly, since there are many thickness design variables in the design parameter vector b. To alleviates this issue an adjoint sensitivity is used to calculate the transmission loss and its sensitivity to the design parameter vector [7]. In this approach, the transmission loss and its sensitivity is calculated in one step without needing to recompute the eigenvalues and eigenvectors every time. The following shows the formulation for the transmission loss sensitivity to a design variable x:

$$\frac{\mathrm{d}TL}{\mathrm{d}x} = \frac{\partial TL}{\partial H}\left[\frac{\partial H}{\partial x} + \sum_{r=1}^{n}\left(\frac{\partial H}{\partial u_r}\frac{\mathrm{d}u_r}{\mathrm{d}x} + \frac{\partial H}{\partial \mu_r}\frac{\mathrm{d}\mu_r}{\mathrm{d}x}\right)\right] \tag{15}$$

In this equation, the first term in the bracket $\frac{\partial H}{\partial x}$ is the explicit derivative of H (resonator assembly frequency response) to a design variable in (5) and their dependencies in (6). For thickness design variables this term is zero. The second term represents the implicit dependence of transmission loss on the design variables and requires the computation of the eigenvectors sensitivity $\frac{\mathrm{d}u}{\mathrm{d}x}$. Utilizing the modal method [7], the sensitivity of the eigenvector is computed according to:

$$\frac{\mathrm{d}u_r}{\mathrm{d}x} = \sum_{j=1}^{l} c_{rj} u_j \tag{16}$$

where l is the number of mode shapes, and

$$c_{rj} = \frac{u_j^T \left(\frac{\mathrm{d}[K]}{\mathrm{d}x} - \mu\frac{\mathrm{d}[M]}{\mathrm{d}x}\right) u_r}{(\mu_r - \mu_j) u_j^T [M] u_j}, \tag{17}$$

In evaluating (17) the derivative of stiffness and mass matrices is calculated using forward finite difference. The derivative of the eigenvalues μ is:

$$\frac{\mathrm{d}\mu}{\mathrm{d}x} = \frac{u^T \left(\frac{\mathrm{d}[K]}{\mathrm{d}x} - \mu\frac{\mathrm{d}[M]}{\mathrm{d}x}\right) u}{u^T [M] u}. \tag{18}$$

The remaining explicit derivatives are evaluated by taking derivative to eigenvectors:

$$\frac{\partial H}{\partial u_r} = \frac{-h_{12}h_{21}}{(\delta v_3 + h_{22})^2}\frac{\partial \delta v_3}{\partial u_r} \tag{19}$$

where

$$\frac{\partial \delta v_3}{\partial u_r} = \frac{(u_r^T A)\delta p + A(u_r^T \delta p)}{(1+i\gamma)\omega_r^2 - \omega^2} \tag{20}$$

and eigenvalues

$$\frac{\partial H}{\partial \mu_r} = \frac{-h_{12}h_{21}}{(\delta v_3 + h_{22})^2}\frac{\partial \delta v_3}{\partial \mu_r} \tag{21}$$

where

$$\frac{\partial \delta v_3}{\partial \mu_r} = -(1+i\gamma)\frac{u_r^T A u_r^T \delta p}{[(1+i\gamma)\omega_r^2 - \omega^2]^2}. \tag{22}$$

Finally the derivatives of explicit term is:

$$\frac{\partial TL}{\partial H} = i\omega \frac{20}{|\beta|^2}\frac{\beta}{\mathrm{Ln}(10)}\frac{\rho a}{2A_{\mathrm{duct}}} \tag{23}$$

6 Verification

The numerical transmission loss function and adjoint sensitivity are verified in the following sections.

6.1 Model Verification

The circular plate was discretized into the meshes shown in Figure 2. The mesh in Figure 2a is constructed by subdividing a master quadrilateral element using the block command in FEAP. The mesh in Figure 2b is constructed using a blending function [15, 17]. Both meshes yield good results in computing the natural modes and transmission loss function. For example, utilizing 768 quadrilateral plate elements in the block mesh, the frequencies of first four modes are calculated and compared to the analytical result(see Table 2).

natural frequency (rad/sec)	ω_1	ω_2	ω_3	ω_4
Percent error	0.591	0.659	0.381	0.743

TABLE 2: Percent error when comparing natural frequencies produced from FEM model and analytical analysis from [9]

Also, for different excitation frequencies the analytical and finite element results for the transmission loss of the baseline resonator (geometric parameters are shown in Table 1) is displayed in Figure 3. In the analytical model three modes are included in the solution. However, the finite element solution uses six modes ($n = 6$) and 972 elements of blocked mesh for one solution and 950 elements of blended mesh for a second solution. An excellent match in transmission loss between the two solutions is observed (see Figure 3). Also, the blended mesh provided a better match to the analytical result than the blocked mesh (see Table 3).

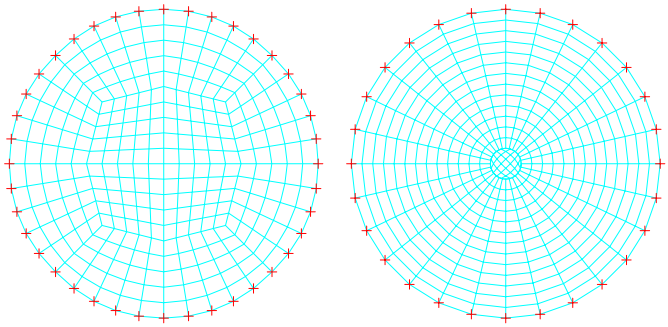

(a) Block mesh (b) Blended mesh

FIGURE 2: Plate finite element mesh

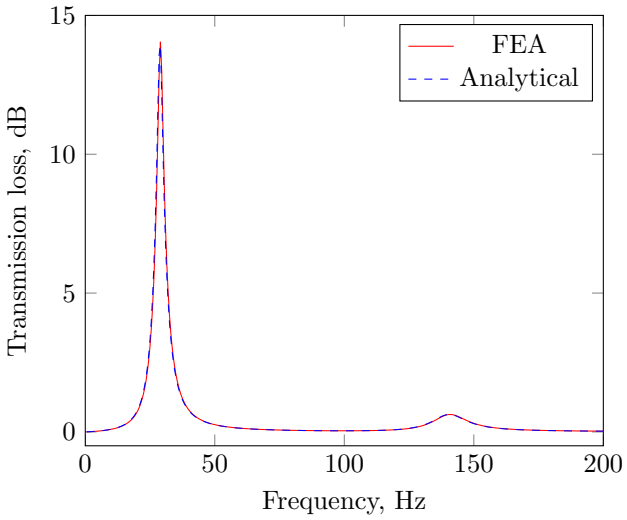

FIGURE 3: Transmission loss function for baseline geometry.

6.2 Sensitivity Verification

To verify the adjoint sensitivity calculations for the flexible plate, forward finite difference results were used to compare the sensitivity results. For this purpose, sensitivity results were

Model	Analytical (4 modes)	Block FEA (972 elements, 6 modes)	Blended FEA (950 elements, 6 modes)
Baseline ΔTL	6.833	7.319	6.875

TABLE 3: Comparison of prediction of ΔTL

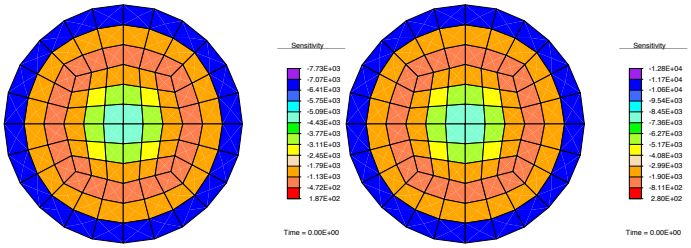

(a) Finite difference sensitivity results for six modes (b) Adjoint sensitivity results for 18 modes

FIGURE 4: Sensitivity of objective for mesh of 108 design variables (elements)

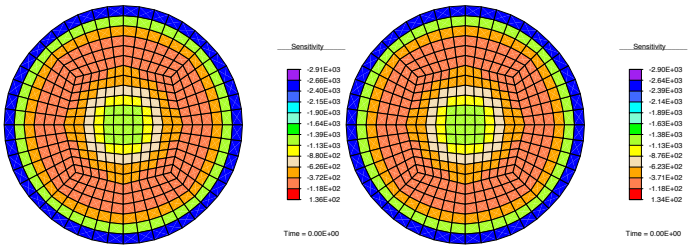

(a) Finite difference sensitivity results for six modes (b) Adjoint sensitivity results for 30 modes

FIGURE 5: Sensitivity of objective for mesh of 432 elements

computed and compared for the baseline plate dimensions (see Section 2).

First, the sensitivity was calculated for the FEA method using a block-type mesh of 108 plate elements and for the finite difference method. The finite difference sensitivity converged using six modes, but 18 modes were required to converge using the adjoint method. The calculated sensitivity for the two methods varied significantly (see Figure 4).

Next, the number of FEA elements was increased from 108 to 432 and both the adjoint method and finite difference method yielded similar results (see Figure 5); therefore, the adjoint sensitivity calculations were verified. The fine mesh increased the accuracy of the finite difference sensitivity results by increasing the accuracy of the response. However, more modes were still required for the adjoint method to converge than for the finite difference method to converge.

6.3 Optimization Results

In this section optimal results for a non-uniform plate thickness for two different Helmholtz resonators with flexible plates are provided: 1) the baseline resonator and 2) a resonator that was previously optimized for maximum transmission loss and minimum resonator size (Optimal Design-1 Resonator). Table 1 shows the resonator and uniform plate dimensions for the two resonators, prior to the optimization of the plate thickness.

The optimization search was completed for two different finite element meshes, a block mesh and a blended mesh. The block-mesh offered consistent element size but lacked radial symmetry. The blended mesh allowed for radial symmetry but lacked element size consistency [17]. A one-to-one ratio of elements and number of design variables was considered for this study. Additionally, initial studies indicated the existence of multiple optimal designs, and the convergence to the optimal design depended on the selection of the initial plate thickness. The results reported here are based on the initial plate thickness that provided the most optimum transmission loss results.

6.3.1 Baseline Resonator Optimization For the baseline resonator, two meshes were considered to discretize the plate, a one-to-one coarse mesh of 108 elements of block type and 148 elements of blended type. The optimization results are shown in Figure 6 for both meshes. By allowing the plate thickness to vary, the transmission loss of the baseline resonator is significantly improved (see Table 4). The results show that the block mesh produces a design with a slightly better transmission loss than the blended mesh, while the blended mesh produces a design with a lighter plate (smaller volume) as compared to the block mesh and the baseline designs.

Resonator	ΔTL	V_f(plate volume)
Baseline with uniform thickness plate	6.833(dB)	$7.6536 \times 10^{-6}(\mathrm{m}^3)$
Baseline with non-uniform thickness plate (block mesh)	8.89(dB)	$7.7723 \times 10^{-6}(\mathrm{m}^3)$
Baseline with non-uniform thickness plate (blended mesh)	8.72(dB)	$7.3274 \times 10^{-6}(\mathrm{m}^3)$

TABLE 4: ΔTL Comparison for uniform and non-uniform thickness plate in the baseline resonator

To study the influence of mesh size on the optimization results, a refined block mesh design utilizing 432 elements (design variables) was used, again for the baseline resonator. The optimization results are shown in Figure 7 and the results are sum-

marized in Table 5. A finer mesh produced an optimal resonator design with an improved transmission loss and a reduced plate volume. In this case, the optimal design favors a more uniform thickness with sections of higher thickness near the boundary.

Resonator	ΔTL	V_f(resonator volume)	number of elements
Baseline with non-uniform thickness plate (block mesh)	8.89(dB)	$7.7723 \times 10^{-6}(\mathrm{m}^3)$	108
Baseline with non-uniform thickness plate (block mesh)	9.08(dB)	$7.6585 \times 10^{-6}(\mathrm{m}^3)$	423

TABLE 5: Influence of the mesh size on weighted transmission loss for the baseline resonator with a non-uniform thickness plate

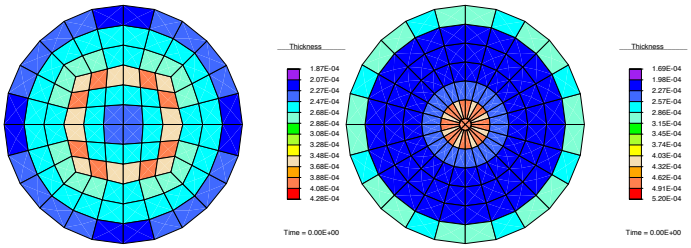

(a) (b)

FIGURE 6: Optimization results of the baseline geometry. (a) block mesh: $\Delta TL = 8.89$ dB (b) blended mesh: $\Delta TL = 8.72$ dB

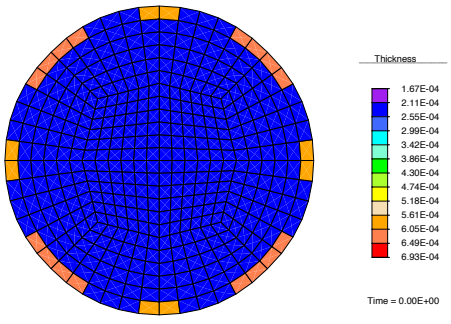

FIGURE 7: Optimization result for the baseline geometry ($\Delta TL = 9.08$ dB)

6.3.2 Level-2 Optimization of the Design-1 Resonator

For the resonator that was previously optimized for maximum transmission loss and minimum resonator size (Optimal Design-1 Resonator) the optimization results for a non-uniform plate thickness are shown in Figure 8 and the transmission loss results are summarized in Table 6. In this case, the blended mesh design improved the transmission loss by only 2 percent while decreasing the plate volume by 4 percent from the Optimal Design-1 Resonator. In the case of block mesh, the optimization reduced the volume of the plate but the amount of transmission loss was reduced.

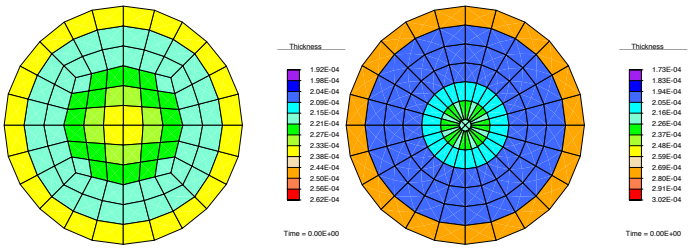

(a) (b)

FIGURE 8: Optimization results of optimal Design-1 geometry. (a) Block mesh: $\Delta TL = 9.05$ dB, (b) Blended mesh: $\Delta TL = 10.48$ dB

Resonator	ΔTL	V_f(resonator volume)	number of elements
Design-1 (level-1)	10.23(dB)	$7.6536 \times 10^{-6}(\mathrm{m}^3)$	N/A
Design-1 (level-2) (block mesh)	9.05(dB)	$7.1857 \times 10^{-6}(\mathrm{m}^3)$	108
Design-1 (level-2) (blended mesh)	10.48(dB)	$7.1653 \times 10^{-6}(\mathrm{m}^3)$	108

TABLE 6: Level-2 optimization results for the Design-1 resonator

7 Conclusion

The use of Helmholtz resonators to attenuate noise requires the selection of a resonator geometry such that noise attenuation is a maximum at the desired frequency. With the goal of improving transmission loss, this work investigated two questions: how much can a flexible endplate with optimized, varying endplate thickness 1) improve the transmission loss of a baseline

resonator with a uniform plate thickness (with no other changes to geometry) and 2) improve the transmission loss of a resonator with a uniform thickness flexible endplate previously optimized for transmission loss and minimum resonator size.

To perform the studies, a finite element model of a resonator end plate of varying thickness was coupled to a single-degree-of-freedom model of the resonator. A sequential quadratic programming algorithm was then used to complete a gradient based optimization search.

By allowing the plate thickness to vary while applying the optimization technique described in this paper, the transmission loss of the baseline resonator was significantly improved (28 percent). If the size of the resonator is not a concern, it is beneficial to perform this optimization. If the resonator has previously been optimized for both maximum transmission loss and minimum resonator volume, extending the optimization to allow for the end plate thickness to vary only increases the transmission loss by 2 percent; therefore, the further optimization is not necessary.

REFERENCES

[1] F Auricchio and RL Taylor. A shear deformable plate element with an exact thin limit. *Computer Methods in Applied Mechanics and Engineering*, 118(3):393–412, 1994.

[2] R.E.D. Bishop and D.C. Johnson. *The mechanics of vibration*. Cambridge Univ. Press, 2011.

[3] RD Cook, DS Malkus, ME Plesha, and RJ Witt. *Concepts and applications of finite element analysis*. Wiley, New York, 2002.

[4] Dan D Davis, George M Stokes, Dewey Moore, and George L Stevens. *Theoretical and experimental investigation of mufflers with comments on engine-exhaust muffler design*. US Government Printing Office, 1954.

[5] Olivier Doaré, Gérald Kergourlay, and Clément Sambuc. Design of a circular clamped plate excited by a voice coil and piezoelectric patches used as a loudspeaker. *Journal of Vibration and Acoustics*, 135(5):051025, 2013.

[6] WH Duan, Chien Ming Wang, and CY Wang. Modification of fundamental vibration modes of circular plates with free edges. *Journal of Sound and Vibration*, 317(3):709–715, 2008.

[7] Raphael T Haftka and Z Gurdal. *Elements of structural optimization*. Kluwer Academic Publishers, Dordrecht, 1992.

[8] Mohammad H Kurdi, G Scott Duncan, and Shahin S Nudehi. Optimal design of a helmholtz resonator with a flexible end plate. *Journal of Vibration and Acoustics*, 136(3):031004, 2014.

[9] Arthur W Leissa. Vibration of plates. Technical report, DTIC Document, 1969.

[10] L Meirovitch. *Principles and techniques of vibrations*, volume 1. Prentice Hall New Jersey, 1997.

[11] S. S. Nudehi, G. S. Duncan, and U. Farooq. Modeling and experimental investigation of a Helmholtz resonator with a flexible plate. ASME Journal of Vibration and Acoustics 2012.

[12] HJ Peters, P Tiso, JFL Goosen, and F van Keulen. A modal-based approach for optimal active modifications of resonance modes. *Journal of Sound and Vibration*, 2014.

[13] Hugo J Peters, Paolo Tiso, Johannes FL Goosen, and Fred van Keulen. Control of the eigensolutions of a harmonically driven compliant structure.

[14] Klaus Schittkowski. NLPQLP: A Fortran implementation of a sequential quadratic programming algorithm with distributed and non-monotone line search-user's guide, version 2.2, 2006.

[15] R. L. Taylor. FEAP - finite element analysis program, 2014.

[16] Samuel Temkin and S Temkin. *Elements of acoustics*. Wiley New York, 1981.

[17] Olgierd Cecil Zienkiewicz and Robert Leroy Taylor. *The finite element method: The Basis*, volume 1. Butterworth-Heinemann, 2000.